

Radial polynomials as alternatives to flat radial basis functions

Fatemeh Pooladi, Hossein Hosseinzadeh*

Department of Mathematics, Persian Gulf University, Bushehr, Iran
Email(s): Fpooladi13@mehr.pgu.ac.ir, hosseinzadeh@pgu.ac.ir

Abstract. Due to the high approximation power and simplicity of computation of smooth radial basis functions (RBFs), in recent decades they have received much attention for function approximation. These RBFs contain a shape parameter that regulates their approximation power and stability but its optimal selection is challenging. To avoid this difficulty, this paper follows a novel and computationally efficient strategy to propose a space of radial polynomials with even degree that well approximates flat RBFs. The proposed space, \mathcal{H}_n , is the shifted radial polynomials of degree $2n$. By obtaining the dimension of \mathcal{H}_n and introducing a basis set, it is shown that \mathcal{H}_n is considerably smaller than \mathcal{P}_{2n} while the distances from RBFs to both \mathcal{H}_n and \mathcal{P}_{2n} are nearly equal. For computation, by introducing new basis functions, two computationally efficient approaches are proposed. Finally, the presented theoretical studies are verified by the numerical results.

Keywords: Smooth radial basis function, radial polynomial, numerical approximation, interpolation.

AMS Subject Classification 2010: 34A34, 65L05.

1 Introduction

Radial basis functions (RBFs) have gained the attention of researchers as they can solve partial differential equations (PDEs) and boundary value problems (BVPs) defined on computational domains with complicated geometries, easily [4, 13]. Also, RBFs are successfully applied for the classification of big data in high-dimensional domains [1, 19, 22]. Infinitely smooth RBFs may yield very accurate numerical results when the unknown function is sufficiently smooth [17, 20]. The accuracy of infinitely smooth RBFs mainly depends on two factors: kernel function, ϕ , and shape parameter, ε . In RBF approximation, the shape parameter should be determined by the user, and the highest accuracy is often obtained at small shape parameters, which may yield unstable results [16, 17]. So a significant number of researchers have focused on the enhancement of stability of flat RBFs, theoretically [5–8, 21]. In [2], Driscoll and

*Corresponding author

Received: 11 November 2023 / Revised: 4 January 2024 / Accepted: 31 January 2024

DOI: 10.22124/jmm.2024.26001.2304

Fornberg showed that the interpolation function converges to a polynomial function that interpolates the same data when ε tends to zero. After that, some researchers have focused on clearing the relation between the polynomials and RBFs and some studies found that the interpolating function obtained by infinitely smooth RBFs converges to polynomial functions when ε tends to zero [9, 11, 14, 18]. The fact that Taylor's expansion of infinitely smooth RBFs contains only even degree of radius, r , motivated us to search for a space of polynomials with even degree for function approximation. Previously, Driscoll and Schaback [2, 18] have used even degree polynomials and introduced the notation of limit interpolating polynomials.

This paper follows a new strategy to introduce a space of radial polynomials and gives some results on the relation between this space and RBFs. For this purpose, we denote the linear space of shifted radial polynomials of degree $2n$ by \mathcal{H}_n . Dimension of \mathcal{H}_n is determined analytically and its basis functions are extracted. One can see that by increasing the size of the base, the distance from the RBFs to \mathcal{H}_n vanishes exponentially. Numerical results show that although $\mathcal{H}_n \subseteq \mathcal{P}_{2n}$, the distances from the RBFs to both linear spaces are nearly equal. So, by our information, \mathcal{H}_n is the smallest subspace of \mathcal{P}_{2n} that smooth RBFs tend to it as fast as possible.

For computation, the usual basis functions of \mathcal{H}_n may lead to unstable numerical results. Therefore, by introducing new basis functions two computationally efficient approaches are proposed which enhance the stability and accuracy of the numerical results significantly. The remaining part of this paper is organized as follows:

The RBFs and their implementation for data approximation are presented in Section 2. Then, in Section 3 the new linear space of radial polynomials, \mathcal{H}_n , is introduced and its dimension and basis functions are obtained. To obtain more stable numerical results and enhance the robustness of the numerical approximation, new basis functions are proposed in Section 4. Some numerical results are presented in Section 5 to verify analytical theories. Finally, the paper is completed by Section 6 including some conclusions and directions for future research.

2 Radial basis functions interpolation

Using RBFs in scattered data approximation was proposed by Hardy [12]. From a point of view, RBFs can be divided into three groups, infinitely smooth, piecewise smooth, and compact support RBFs. Some well-known RBFs are listed in Table 1. Suppose given data of the form (\mathbf{x}_i, u_i) for $i = 1, 2, \dots, N$ where $\mathbf{x}_i \in \Omega \subseteq \mathbb{R}^d$ and $u_i \in \mathbb{R}$. We seek for an interpolant $\bar{u}(\mathbf{x})$ which satisfies

$$\bar{u}(\mathbf{x}_i) = u_i, \quad i = 1, 2, \dots, N. \quad (1)$$

In RBF interpolation approach, $\bar{u}(\mathbf{x})$ is a linear function of RBFs $\phi(r_1(\mathbf{x})), \phi(r_2(\mathbf{x})), \dots, \phi(r_N(\mathbf{x}))$ as

$$\bar{u}(\mathbf{x}) = \sum_{i=1}^N \lambda_i \phi(r_i(\mathbf{x})), \quad (2)$$

such that λ_i are constants and $r_i(\mathbf{x}) = \|\mathbf{x} - \mathbf{x}_i\|$. In fact, interpolant \bar{u} belongs to the linear space S spanned by RBFs $\phi(r_1(\mathbf{x})), \phi(r_2(\mathbf{x})), \dots, \phi(r_N(\mathbf{x}))$. It means

$$\bar{u} \in S = \langle \phi(r_1(\mathbf{x})), \phi(r_2(\mathbf{x})), \dots, \phi(r_N(\mathbf{x})) \rangle. \quad (3)$$

Table 1: Some important RBFs presented in the literature.

RBF	name	function
infinitely smooth	Gaussian (GA)	$\exp(-\varepsilon^2 r^2)$
	Multiquadric (MQ)	$\sqrt{1 + \varepsilon^2 r^2}$
	Inverse Multiquadric (IMQ)	$1/\sqrt{1 + \varepsilon^2 r^2}$
	Inverse Quadric (IQ)	$1/(1 + \varepsilon^2 r^2)$
piecewise smooth	Thin plate spline (TPS)	$r^{2n} \ln(r)$
	Poly-harmonic Spline (PHS)	r^{2n+1}
compactly support	Wendland C^0	$(1 - r)_+^2$
	Wendland C^2	$(1 - r)_+^4 (1 + 4r)$

The value of RBF $\phi(r_i(\mathbf{x}))$ depends on the kind of RBFs that are used, the distance from the input data \mathbf{x} to the collocation point \mathbf{x}_i and the shape parameter, ε . Eq. (2) can be stated as a system of linear equations

$$\Phi \lambda = \mathbf{b}, \tag{4}$$

where $\Phi[i, j] = \phi(r_i(\mathbf{x}_j))$, $\lambda = [\lambda_1, \lambda_2, \dots, \lambda_N]^T$, and $\mathbf{b} = [\bar{u}(\mathbf{x}_1), \bar{u}(\mathbf{x}_2), \dots, \bar{u}(\mathbf{x}_N)]^T$. This system is non singular when positive definite RBFs (such as GA RBF) with constant shape parameters are used [3, 20]. It has been shown that the interpolant function admits spectral convergence when infinitely smooth RBFs are applied [20]. However, the accuracy and the stability of these RBFs depend on the number of data points and the value of ε [15, 17, 20]. It is well-known that interpolation function \bar{u} converges exponentially to a polynomial function when the shape parameter, ε , is sufficiently small or N is sufficiently large [2, 10].

3 Linear space of radial polynomials

This section introduces the new linear space of radial polynomials to be used as an alternative for linear space S introduced in Eq. (3). The new linear space is free of the shape parameter.

3.1 Motivation and the proposed linear space

As mentioned in Eqs. (2) and (3) the interpolant \bar{u} belongs to linear space S . Considering Taylor's expansion of a smooth RBF, $\phi(r_i)$, we have

$$\phi(r_i) \simeq f_{n_i}(r_i) = 1 + c_1 \varepsilon^2 r_i^2 + c_2 \varepsilon^4 r_i^4 + \dots + c_{n_i} \varepsilon^{2n_i} r_i^{2n_i}. \tag{5}$$

It is worth to mention that in machine computation this expansion is truncated when its terms become smaller than machine precision. So, the Taylor's expansion ends at machine precision, and in practice, it does not go to infinity. By this motivation, instead of S , we consider the space generated by polynomials $f_{n_i}(r_i)$, as follows

$$\mathcal{H} = \langle f_{n_1}(r_1), f_{n_2}(r_2), \dots, f_{n_N}(r_N) \rangle. \tag{6}$$

To avoid the complexity of computation in (6), the space \mathcal{H}_n is proposed as follows which contains shifted radial polynomials of degree $2n$:

$$\mathcal{H}_n = \langle r_1^{2n}, r_2^{2n}, \dots, r_N^{2n} \rangle; n = \max\{n_1, \dots, n_N\}. \quad (7)$$

Using \mathcal{H}_n for approximation has less computational cost than \mathcal{H} , and in the following, it is proved that in the case where \mathcal{H}_n is full rank then $\mathcal{H} \subseteq \mathcal{H}_n$.

3.2 Relation between \mathcal{H}_n and \mathcal{H}

From Eqs. (5) and (7) we find that \mathcal{H} and \mathcal{H}_n both include polynomials of degree less than or equal to $2n$. In this subsection, it is proved by a theorem that, \mathcal{H} is embedded in \mathcal{H}_n if \mathcal{H}_n is full rank. Note that \mathcal{H}_n is full rank if $r_0^{2n} \in \mathcal{H}_n$ for all $\mathbf{x}_0 \in \Omega$.

Lemma 1. *If \mathcal{H}_n is full rank then \mathcal{H}_{n-1} is also full rank for $n \geq 1$.*

Proof. Suppose \mathcal{H}_n is full rank, so for any computational point $\mathbf{x}_0 \in \mathbb{R}^d$ there are coefficients $\lambda_1, \dots, \lambda_N$ in \mathbb{R} such that

$$r_0^{2n} = \sum_{i=1}^N \lambda_i r_i^{2n}. \quad (8)$$

Now imposing Laplace operator, ∇^2 , on both sides of Eq. (8) results in

$$r_0^{2n-2} = \sum_{i=1}^N \lambda_i r_i^{2n-2}, \quad (9)$$

which shows that \mathcal{H}_{n-1} is also full rank. □

Corollary 1. *If \mathcal{H}_n is full rank then \mathcal{H}_j also is full rank for each $j \leq n$.*

Proof. It can be proved by Lemma 1 and induction on j when j decreases from n to 1 step by step. □

Lemma 2. *If \mathcal{H}_n is full rank then $\mathcal{H}_{n-1} \subseteq \mathcal{H}_n$ for $n \geq 1$.*

Proof. Let \mathbf{x}_0 be a computational point in \mathbb{R}^d . Therefore

$$r_0^{2n-2} = \frac{1}{4n^2} \nabla^2 r_0^{2n} = \frac{1}{4n^2} \lim_{h \rightarrow 0} \frac{1}{h^2} \left(\sum_{j=0:2d} \lambda_j r_0^{2n}(x + h\mathbf{v}_j) \right), \quad (10)$$

where λ_j and \mathbf{v}_j are appropriate finite difference coefficients and vectors, respectively for $j = 0, 1, 2, \dots, 2d$. Since polynomials $r_0^{2n}(x_0 + h\mathbf{v}_j)$ belong to \mathcal{H}_n and \mathcal{H}_n is a closed space (because it has finite dimension), the limit presented on the right-hand side of Eq. (10) also belongs to \mathcal{H}_n and consequently $r_0^{2n-2} \in \mathcal{H}_n$. So, $\mathcal{H}_{n-1} \subseteq \mathcal{H}_n$. □

Corollary 2. *If \mathcal{H}_n is full rank, then $\mathcal{H}_j \subseteq \mathcal{H}_n$ for $j \leq n$.*

Proof. It can be proved by Lemma 2 and induction on j when it decreases from n to 1, step by step. □

Now the important theorem can be achieved from the last corollary.

Theorem 1. *If \mathcal{H}_n is full rank, then $\mathcal{H} \subseteq \mathcal{H}_n$.*

Proof. From Corollary 2 we have $\mathcal{H}_0 \subseteq \mathcal{H}_1 \subseteq \dots \subseteq \mathcal{H}_{n-1} \subseteq \mathcal{H}_n$ where it leads

$$\mathcal{H}_0 + \mathcal{H}_1 + \dots + \mathcal{H}_n = \mathcal{H}_n,$$

and consequently $f_n(r_i) \in \mathcal{H}_n$ for $i = 1, 2, \dots, N$, and $\mathcal{H} \subseteq \mathcal{H}_n$. \square

3.3 A base for \mathcal{H}_n

Now we are going to introduce a base for \mathcal{H}_n . From Theorem 1 we have $\mathcal{H} \subseteq \mathcal{H}_n$ when \mathcal{H}_n is full rank and consequently a base of \mathcal{H}_n is also a base of \mathcal{H} , when dimension of \mathcal{H} and \mathcal{H}_n are equal. Note that elements of \mathcal{H}_n are radial polynomials of degree $2n$ and the dimension of \mathcal{H}_n is bounded by the dimension of polynomials of degree less than or equal to $2n$, denoted by \mathcal{P}_{2n} . We will see that the dimension of \mathcal{H}_n is significantly smaller than the dimension of \mathcal{P}_{2n} for $d \geq 2$.

Lemma 3. *If $r^2 = \|\mathbf{x}\|^2$ and $m \leq n$, then the dimension of the linear space spanned by elements of set $\{r^2 \mathcal{P}_{m-1} - \mathcal{P}_m\}$, i.e. $\langle r^2 \mathcal{P}_{m-1} - \mathcal{P}_m \rangle$, is equal to*

$$\binom{m+d-2}{m-1} = \frac{(m+d-2)!}{(m-1)!(d-1)!}. \quad (11)$$

Proof. Since $r^2 \in \mathcal{P}_2$, $r^2 \mathcal{P}_{m-1}$ is a set of polynomials of degree less than or equal to $m+1$ which have factor r^2 in their components. Subtracting \mathcal{P}_m from this set, only polynomials of degree $m-1$ remain which are multiplied by r^2 , i.e.

$$\langle r^2 \mathcal{P}_{m-1} - \mathcal{P}_m \rangle = r^2 \langle \mathcal{P}_{m-1} - \mathcal{P}_{m-2} \rangle.$$

Polynomial basis functions of $\langle \mathcal{P}_{m-1} - \mathcal{P}_{m-2} \rangle$ satisfy condition

$$\prod_{k=1:d} x_k^{\alpha_k} \quad s.t. \quad \sum_{k=1:d} \alpha_k = m-1,$$

where x_k is k -th component of \mathbf{x} for $k = 1, 2, \dots, d$. The number of these basis functions can be calculated via Eq. (11). \square

Theorem 2. *Dimension of \mathcal{H}_n is less than or equal to*

$$h(n) = 2 \sum_{i=0:n-1} \binom{i+d-1}{i} + \binom{n+d-1}{n},$$

for $n \geq 2$.

Proof. The proof can be done via induction. For $n = 0$, we have $\mathcal{H}_0 = \{1\}$ and $\dim(\mathcal{H}_0) = 1$. For $n = 1$, if \mathbf{x}_0 is a computational point in \mathbb{R}^d and $\mathbf{x} = (x_1, x_2, \dots, x_d)$ then

$$r_0^2 = \|\mathbf{x} - \mathbf{x}_0\|^2 = (\mathbf{x} - \mathbf{x}_0)(\mathbf{x} - \mathbf{x}_0)^T = \|\mathbf{x}_0\|^2 - 2\mathbf{x}_0\mathbf{x}^T + \|\mathbf{x}\|^2 = c_0 + \sum_{k=1:d} c_k x_k + r^2, \quad (12)$$

where c_0, c_1, \dots, c_d are constant numbers depending on \mathbf{x}_0 . Then, \mathcal{H}_1 has one base of degree zero, d basis of degree one, and one base of degree two.

For $n \geq 2$, by Eq. (12) we have

$$r_0^{2n} = (r_0^2)^n = (c_0 + \sum_{k=1:d} c_k x_k + r^2)^n = \sum_{\sum \alpha_k + \beta \leq n} c(\alpha_1, \alpha_2, \dots, \alpha_d, \beta) \prod_{k=1:d} x_k^{\alpha_k} r^{2\beta},$$

where $c(\alpha_1, \alpha_2, \dots, \alpha_d, \beta)$ are constant numbers depending on $\alpha_1, \alpha_2, \dots, \alpha_d$ and β . The last equality shows the basis functions of \mathcal{H}_n are in the form

$$\prod_{k=1:d} x_k^{\alpha_k} r^{2\beta} \quad s.t. \quad \sum \alpha_k + \beta \leq n.$$

To count basis functions of \mathcal{H}_n , we split \mathcal{H}_n into disjoint subsets and count their basis functions separately by using Lemma 3. These disjoint subsets are $\mathcal{P}_n, \langle \mathcal{P}_{n-1}r^2 - \mathcal{P}_n \rangle, \langle \mathcal{P}_{n-2}r^4 - \mathcal{P}_{n-1}r^2 \rangle, \dots, \langle \mathcal{P}_0r^{2n} - \mathcal{P}_1r^{2n-1} \rangle$ which they lead to

$$\begin{aligned} \mathcal{H}_n &= \sum_{i=0}^n \mathcal{P}_{n-i}r^{2i} = \mathcal{P}_n + \sum_{i=1:n} \langle \mathcal{P}_{n-i}r^{2i} - \mathcal{P}_{n-i-1}r^{2(i-1)} \rangle \\ &= \mathcal{P}_n + \sum_{i=1:n} \langle \mathcal{P}_{n-i}r^2 - \mathcal{P}_{n-i-1} \rangle r^{2(i-1)}, \end{aligned} \tag{13}$$

and by Lemma 3 we have

$$\begin{aligned} \dim(\mathcal{H}_n) &= \dim(\mathcal{P}_n) + \sum_{i=1:n} \dim(\langle \mathcal{P}_{n-i} - \mathcal{P}_{n-i-1} \rangle) \\ &= \sum_{i=0:n} \binom{i+d-1}{i} + \sum_{i=1:n} \binom{n-i+d-1}{n-i} \\ &= 2 \sum_{i=0:n-1} \binom{i+d-1}{i} + \binom{n+d-1}{n}. \end{aligned} \tag{14}$$

□

Theorem 2 presents a constructive algorithm to obtain the basis functions of \mathcal{H}_n . Figure 1 shows these basis functions for $d = 1, 2$ and 3 where in this figure $r^2 = \|\mathbf{x}\|^2$.

From Theorem 2 dimension of \mathcal{H}_n is equal to

$$h(n) = \begin{cases} 2n + 1, & \text{if } d = 1, \\ (n + 1)^2, & \text{if } d = 2, \\ (n + 1)(n + 2)(2n + 3)/6, & \text{if } d = 3, \end{cases} \tag{15}$$

when it is full rank. Also from Theorem 1 dimension of linear space \mathcal{H} is less than or equal to $h(n)$. It is notable that dimension of \mathcal{H}_n already is calculated experimentally in [2]. The experiment results presented in [2] confirm Theorem 2. From the above statements, some important relations can be extracted between polynomial linear spaces \mathcal{H}_n and \mathcal{P}_n which are summarized in the following corollary.

Corollary 3. Let \mathcal{H}_n be the linear space of radial polynomials of degree $2n$ and \mathcal{P}_n be the linear space of polynomials of degree less than or equal to n . If \mathcal{H}_n is full rank then the following items hold.

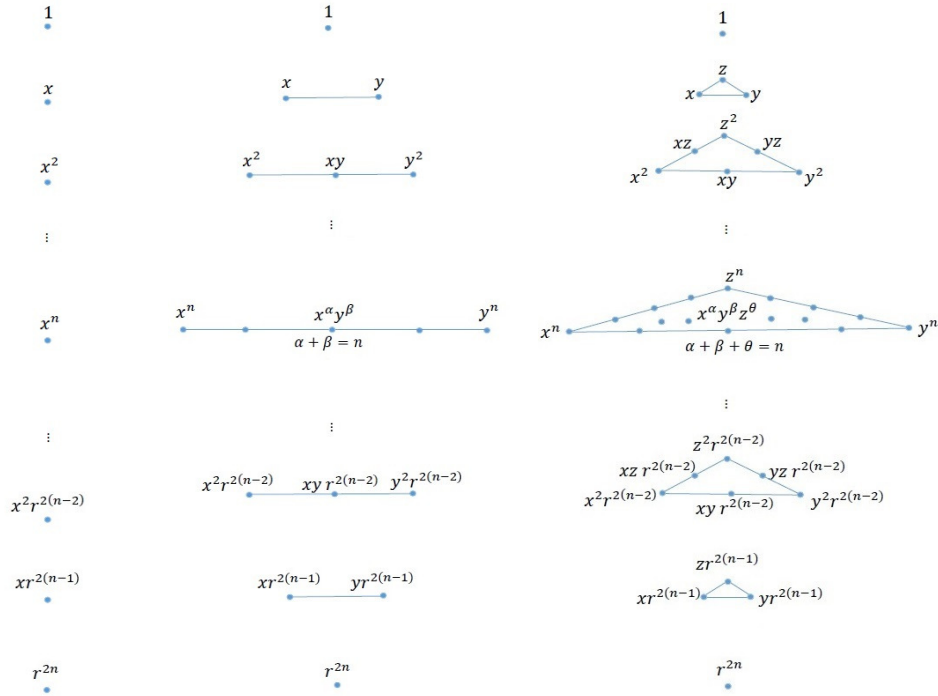


Figure 1: Diagram of basis functions of \mathcal{H}_n for $d = 1$ (left), $d = 2$ (middle), and $d = 3$ (right).

- $\mathcal{P}_n \subset \mathcal{H}_n \subseteq \mathcal{P}_{2n}$,
- $\dim(\mathcal{H}_n) = \dim(\mathcal{P}_n) + \dim(\mathcal{P}_{n-1})$,
- $\mathcal{H}_n = \mathcal{P}_{2n}$ for $d = 1$,
- $\mathcal{P}_{n+1} \not\subseteq \mathcal{H}_n \subset \mathcal{P}_{2n}$ for $d \geq 2$.

4 Computationally efficient basis functions for \mathcal{H}_n

Basis functions $p_i = r_i^{2n}$, presented in Eq. (6), have a simple form but they are not computationally efficient, i.e. despite their simplicity, they are not numerically stable. Generally, to enhance the stability, the basis functions can be normalized by mapping the distance function r_i to $[0, 1]$ as

$$r_i = r_i / \max_{x \in \Omega} \{r_i\}.$$

By this normalization, the basis functions are mapped to $[0, 1]$ and this enhances the stability. Note that the normalized basis functions, p_i , vanish close to the center point, \mathbf{x}_i , and increase rapidly close to some boundary points far from the center point, specially when n is large. For instance, $p_i \leq 10^{-12}$ for $r_i < 0.5$

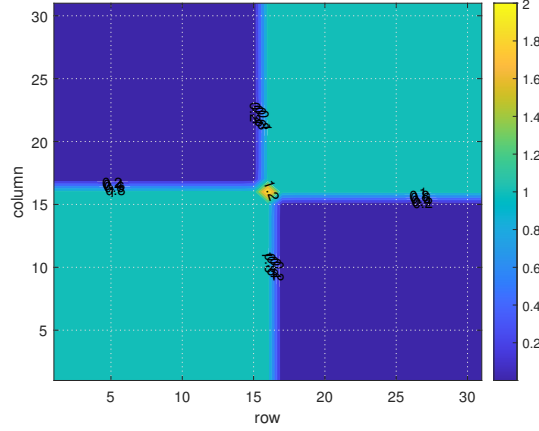


Figure 2: Contour lines of elements of matrix $\mathbf{A} = \Phi^T \Phi$ for polynomial basis functions p_i .

and $p_i = 1$ at $r_i = 1$ when $n \geq 20$. In this situation, two basis functions p_i and p_j are strongly dependent when there is a point $\mathbf{y} \in \Omega$ satisfying

$$\arg \max_{\mathbf{x} \in \Omega} \{\|\mathbf{x}_i - \mathbf{x}\|\} = \mathbf{y} = \arg \max_{\mathbf{x} \in \Omega} \{\|\mathbf{x}_j - \mathbf{x}\|\}.$$

Since the contour lines of a matrix visually represent the values of its elements, to check the dependency of the basis functions, contour lines of elements of matrix $\mathbf{A} = \Phi^T \Phi$ are shown in Figure 2 when $\mathbf{x}_i = (i-1)/2n$ for $i = 1, 2, \dots, 2n+1$ and $n = 15$. Since

$$\mathbf{A}[i, j] = (\Phi[:, i]) \cdot (\Phi[:, j]) = \sum_{k=1:N} \phi(r_i(\mathbf{x}_k)) \phi(r_j(\mathbf{x}_k)),$$

matrix \mathbf{A} contains dot products of columns of matrix Φ . Here, $\Phi[:, i]$ is i -th column of matrix Φ . Therefore $\mathbf{A}[i, j]$ shows a dependency (or similarity) between p_i and p_j . When the bases are orthonormal, the main diagonal entries of \mathbf{A} , will be one, and other elements will be zero. According to Figure 2, one can see $\mathbf{A}[i, j] \simeq 1$ for $1 \leq i, j \leq n$ and $n+2 \leq i, j \leq 2n+1$ for one-dimensional domains. This shows a high dependency between the basis functions. This dependency results in unstable numerical results and a large value of condition number, defined as

$$\text{cond}(\Phi) = \|\Phi\| \|\Phi^{-1}\|.$$

In the following subsections, two approaches are proposed to reduce the dependency and enrich the stability of numerical results by introducing some new basis functions for \mathcal{H}_n .

4.1 Semi-cardinal basis functions

To find more stable basis functions, we focus on basis functions that are similar to the cardinal functions, taking 1 at a center point and 0 at the other nodes. This property enhances the stability by resulting in a

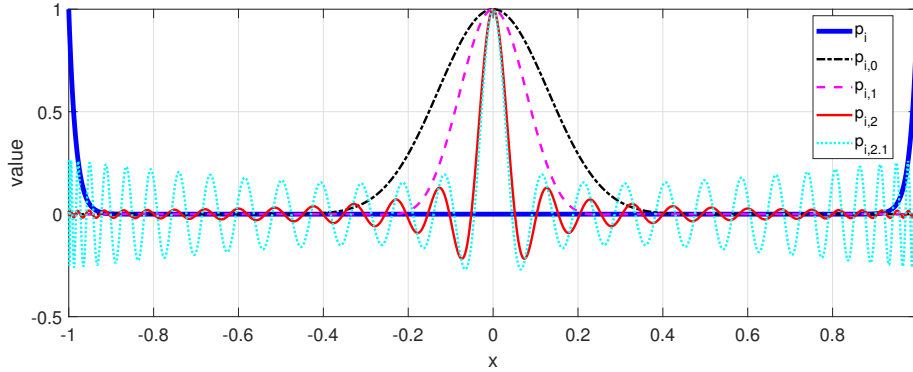


Figure 3: Cross sections of polynomials $p_{i,\tau} = \prod_{k=1:n}(r_i^2 - t_k^\tau)$ for $\tau = 0, 1, 2, 2.1$, where the center point is 0 and $n = 30$. $p_{i,\tau}$ takes 1 at the center point and vanishes at points far from the center for $\tau \leq 2$.

diagonal-like coefficient matrix Φ . For this goal, we introduce basis functions

$$p_{i,\alpha} = \prod_{k=1:n} (r_i^2 - \alpha_k^2),$$

for $i = 1, 2, \dots, h(n)$ and some positive vector $\alpha = [\alpha_1^2, \alpha_2^2, \dots, \alpha_n^2]$. According to Theorem 2, these basis functions are applicable in each dimension. Basis functions, $p_{i,\alpha}$ are polynomial functions with roots $\alpha_1, \alpha_2, \dots, \alpha_n$. Note that, $p_i = p_{i,\mathbf{0}}$ where $\mathbf{0}$ is the zero vector. A cross-section of the basis function is plotted in Figure 3 where the center point is 0 and $\alpha_k^2 = t_k^\tau$ for $\tau = 0, 1, 2, 2.1$ and t_k is the k th positive root of Chebyshev polynomial of the first kind of degree $2n + 1$, i.e.

$$t_k = \cos\left(\frac{2k-1}{4n+2}\pi\right).$$

It is easy to find from Figure 3 that $\tau > 2$ does not yield flat functions for the points far from the center, so, τ should be restricted with $\tau \leq 2$. Therefore, we propose the following functions as the semi-cardinal basis of \mathcal{H}_n :

$$p_{i,\tau} = \prod_{k=1:n} (r_i^2 - t_k^\tau); \quad \tau \in [0, 2]. \tag{16}$$

To test the stability of the proposed basis functions, the condition number of the coefficient matrix, Φ , is presented in Figure 4 for one-dimensional domains and $\tau = 0, 1$ and 2. In Figure 4 center points are chosen as $\mathbf{x}_i = (i-1)/2n$ for $i = 1, 2, \dots, 2n+1$ where $n = 15$. From Figure 4, the condition number of the coefficient matrix for $p_{i,2}$ is smaller than the others, especially GA RBF with shape parameter $\epsilon = 1$. So, this result suggests the use of basis functions $p_{i,2}$ to enhance the numerical stability in interpolation. To check the dependency of basis functions $p_{i,2}$ and $p_{j,2}$ for $i, j = 1, 2, \dots, h(n)$, contour lines of elements of matrix $\mathbf{A} = \Phi^T \Phi$ are shown in Figure 5. From this figure, large elements of the matrix are located close to its diagonal, and small elements are far away. Therefore, the basis functions $p_{i,2}$ and $p_{j,2}$ are nearly independent when the distance between their center points is sufficiently large. This property of the semi-cardinal basis functions enhances the stability of numerical results, especially for large n .

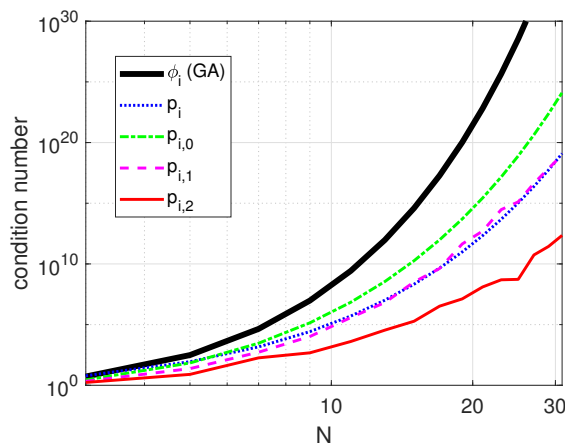


Figure 4: Condition number of the coefficient matrix, Φ , for GA RBF with $\varepsilon = 1$ and polynomial basis functions $p_i, p_{i,0}, p_{i,1}$ and $p_{i,2}$. The condition number of $p_{i,2}$ is smaller than that of GA RBF and p_i for large values of n .

4.2 Regularized basis functions

Although the new basis functions $p_{i,2}$ enhance the stability, they all are polynomials of degree $2n$. This fact reduces the accuracy of approximation (2) for large values of n because polynomials with lower degrees do not appear in the set of basis functions. To overcome this drawback, basis functions with lower degrees should be replaced with some basis functions of degree $2n$. Therefore, a set of regularized basis functions containing polynomials of degree $0, 2, 4, \dots, 2n$ are proposed as follows

$$q_{1,2} = 1, \quad q_{i,2} = \prod_{k=1:j} (r_i^2 - t_k^2), \quad (17)$$

for $i = h(j-1) + 1, h(j-1) + 2, \dots, h(j)$ where $j = 1, 2, \dots, n$ and $t_k = \cos((2k-1)\pi/(4j+2))$. The proposed regularized basis functions can be presented in expanded form below

$$\begin{aligned} q_{1,2} &= 1, \\ q_{i,2} &= (r_i^2 - t_1^2), \quad i = 2, 3, \dots, h(1), \quad t_1 = \cos\left(\frac{1}{6}\pi\right), \\ q_{i,2} &= \prod_{k=1:2} (r_i^2 - t_k^2), \quad i = h(1) + 1, h(1) + 2, \dots, h(2), \quad t_k = \cos\left(\frac{2k-1}{10}\pi\right), \\ &\vdots \\ q_{i,2} &= \prod_{k=1:n} (r_i^2 - t_k^2), \quad i = h(n-1) + 1, h(n-1) + 2, \dots, h(n), \quad t_k = \cos\left(\frac{2k-1}{4n+2}\pi\right), \end{aligned}$$

where the function in the first row is the base of \mathcal{H}_0 , functions in the second row are the basis of \mathcal{H}_1 , and so on. Note that the same strategy can be used for the other basis functions to obtain regularized basis functions. For instance, regularized monomial basis functions can be obtained from p_i for $i =$

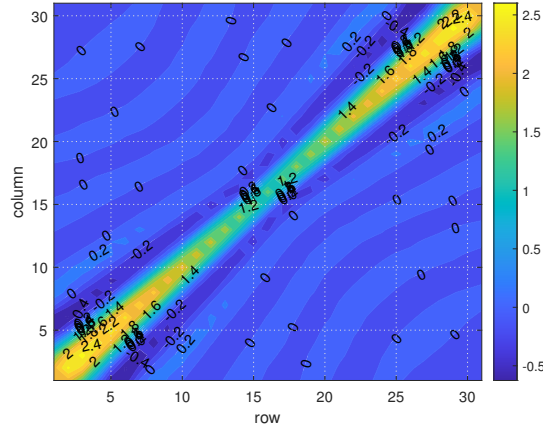


Figure 5: Contour lines of elements of matrix \mathbf{A} for basis functions $p_{i,2}$.

$h(j-1) + 1, h(j-1) + 2, \dots, h(j)$ and $j = 1, 2, \dots, n$ as

$$q_1 = 1 \quad , \quad q_i = r_i^{2j}. \tag{18}$$

Numerical experiments presented in Subsection 5.2 show the ability and efficiency of the new regularized polynomial basis functions for approximation.

5 Numerical verification

This section contains some numerical results to verify and confirm our theoretical study presented in the previous sections. At first, the ability of the proposed new linear space, \mathcal{H}_n , is analyzed numerically. For this purpose, the distance from some smooth RBFs to linear spaces \mathcal{H}_n , \mathcal{P}_{2n-1} and \mathcal{P}_{2n} are presented in Subsection 5.1. In Subsection 5.2 the performance of the proposed basis functions are investigated and the approximation power and stability of the proposed basis functions are compared with GA RBFs and polynomials. The results on irregular domains are also presented and both two and three-dimensional problems are considered.

5.1 The distance from smooth RBFs to \mathcal{H}_n

The distance from RBF $\phi_0(\mathbf{x}) = \phi(\mathbf{x} - \mathbf{x}_0)$ to \mathcal{H}_n for a fixed point $\mathbf{x}_0 \in \Omega$ is defined as

$$dis(\phi_0, \mathcal{H}_n) = \min_{p \in \mathcal{H}_n} \|\phi_0 - p\|_2 = \|\phi_0 - p_0\|_2, \tag{19}$$

where $p_0 \in \mathcal{H}_n$ satisfies $\int_{\Omega} (\phi_0(\mathbf{x}) - p_0(\mathbf{x}))p(\mathbf{x})d\mathbf{x} = 0$ for all $p \in \mathcal{H}_n$. If p_0 is expanded by polynomial basis functions $p_1, p_2, \dots, p_{h(n)}$ of \mathcal{H}_n as $p_0 = \sum_{k=1:h(n)} \alpha_k p_k$, then the unknown coefficients $\alpha_1, \alpha_2, \dots, \alpha_{h(n)}$ are determined by solving system of linear equations $\mathbf{B}\boldsymbol{\alpha} = \mathbf{b}$, where

$$\mathbf{B}[i, j] = \int_{\Omega} p_i(\mathbf{x})p_j(\mathbf{x})d\mathbf{x} \quad , \quad \boldsymbol{\alpha}[i] = \alpha_i \quad , \quad \mathbf{b}[i] = \int_{\Omega} p_i(\mathbf{x})\phi_0(\mathbf{x})d\mathbf{x} \quad , \tag{20}$$

Table 2: The distance from smooth RBF $\phi(\mathbf{x} - \mathbf{x}_0)$ to linear spaces \mathcal{H}_n , \mathcal{P}_{2n-1} and \mathcal{P}_{2n} where $\mathbf{x}_0 = (0, 0)$, $\varepsilon = 1/2$ and $\mathbf{x} \in [-1, 1]^2$.

RBF	Linear space	n					
		2	3	4	5	6	7
GA	\mathcal{H}_n	$4.28e-4$	$1.32e-5$	$3.26e-7$	$6.71e-9$	$1.19e-10$	$2.01e-12$
	\mathcal{P}_{2n-1}	$1.06e-2$	$4.20e-4$	$1.25e-5$	$3.00e-7$	$6.02e-9$	$1.04e-10$
	\mathcal{P}_{2n}	$4.20e-4$	$1.25e-5$	$3.00e-7$	$6.01e-9$	$1.04e-10$	$2.00e-12$
IMQ	\mathcal{H}_n	$5.18e-4$	$4.57e-5$	$4.12e-6$	$3.79e-7$	$3.54e-8$	$3.33e-9$
	\mathcal{P}_{2n-1}	$6.21e-3$	$5.06e-4$	$4.31e-5$	$3.78e-6$	$3.38e-7$	$3.08e-8$
	\mathcal{P}_{2n}	$5.06e-4$	$4.31e-5$	$3.78e-6$	$3.38e-7$	$3.08e-8$	$2.84e-9$
MQ	\mathcal{H}_n	$1.24e-4$	$7.86e-6$	$5.53e-7$	$4.16e-8$	$3.30e-9$	$2.70e-10$
	\mathcal{P}_{2n-1}	$2.46e-3$	$1.21e-4$	$7.41e-6$	$5.07e-7$	$3.72e-8$	$2.87e-9$
	\mathcal{P}_{2n}	$1.21e-4$	$7.42e-6$	$5.07e-7$	$3.72e-8$	$2.87e-9$	$2.30e-10$
IQ	\mathcal{H}_n	$1.52e-3$	$1.53e-4$	$1.53e-5$	$1.53e-6$	$1.54e-7$	$1.55e-8$
	\mathcal{P}_{2n-1}	$1.52e-2$	$1.48e-3$	$1.43e-4$	$1.40e-5$	$1.37e-6$	$1.34e-7$
	\mathcal{P}_{2n}	$1.48e-3$	$1.43e-4$	$1.40e-5$	$1.37e-6$	$1.34e-7$	$1.31e-8$

for $i, j = 1, 2, \dots, h(n)$. The distance between ϕ_0 and \mathcal{H}_n is calculated for some RBFs and are reported in Table 2 where $\varepsilon = 1/2$, $\mathbf{x}_0 = (0, 0)$, $\Omega = [-1, 1]^2$ and $n \leq 7$. The studied RBFs in this subsection are

- GA RBF, $\phi(r) = \exp(-\varepsilon^2 r^2)$,
- IMQ RBF, $\phi(r) = (1 + \varepsilon^2 r^2)^{-1/2}$,
- MQ RBF, $\phi(r) = (1 + \varepsilon^2 r^2)^{1/2}$,
- IQ RBF, $\phi(r) = (1 + \varepsilon^2 r^2)^{-1}$.

From this table, the distance vanishes exponentially when n increases and it is smaller than 10^{-8} for $n > 7$. Also, results of Table 2 reveal that the GA RBF is closer to the new linear space than the other RBFs. Moreover, the distance from the RBFs to linear spaces \mathcal{P}_{2n-1} and \mathcal{P}_{2n} is also calculated and presented in Table 2. From numerical results of Table 2, we have

$$dis(\phi_0, \mathcal{P}_{2n}) \simeq dis(\phi_0, \mathcal{H}_n) < dis(\phi_0, \mathcal{P}_{2n-1}),$$

while $\mathcal{H}_n \subset \mathcal{P}_{2n}$ and the dimension of \mathcal{H}_n is significantly smaller than the dimensions of \mathcal{P}_{2n-1} and \mathcal{P}_{2n} for large values of n . This fact reveals that \mathcal{H}_n is the smallest subspace of \mathcal{P}_{2n} which the distance from the smooth RBFs to it tends to zero as fast as possible when n increases.

5.2 Investigating the efficiency of \mathcal{H}_n

In this subsection, to investigate the approximation power the \mathcal{H}_n , the interpolation problem is solved with the different proposed base of \mathcal{H}_n ($p_i, p_{i,2}, q_i$ and $q_{i,2}$) and is compared with GA RBFs and common polynomials in 2D ($x^i y^j; i, j = 0, 1, \dots, 2n$) and 3D ($x^i y^j z^k; i, j, k = 0, 1, \dots, 2n$). The ε varies from 10^{-2} to

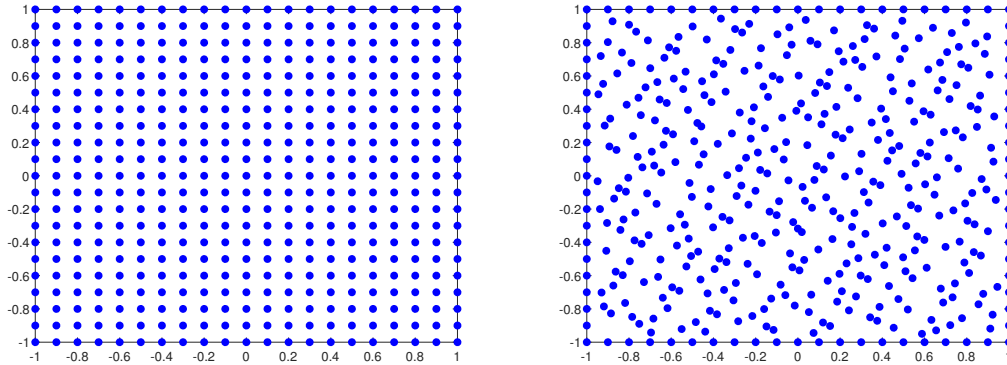


Figure 6: Left: Uniform grid points (UGP) in the square computational domain. Right: Halton points (HP) in the square computational domain.

10^2 . The domain of study in 2D is regular (the square) and irregular (the star-shape) and the distribution of points are the uniform grid points (UGP) and Halton points (HP). Especially in the 3D, the domain is cubic $[-1, 1]^3$, and the distribution of points is HP. It is important to mention that results for MQ, IMQ, and IQ RBFs are the same as GA RBF, so we just report the result of GA RBF.

5.2.1 2D regular and irregular domains

Consider the following functions for interpolation on $\Omega = [-1, 1]^2$:

$$u_1(\mathbf{x}) = \sin(x + y) \quad \text{and} \quad u_2(\mathbf{x}) = \tanh(x + y).$$

Center points are considered in both UGP and HP forms in Ω as is shown in Figure 6. The root mean square error (RMSE) of interpolation is calculated as

$$\text{error} = \frac{1}{\sqrt{N}} \sqrt{\sum_{i=1:N} (u(\mathbf{y}_i) - \bar{u}(\mathbf{y}_i))^2}, \quad (21)$$

where u and \bar{u} are analytical and numerical solutions, respectively and \mathbf{y}_i is selected in $[-1, 1]^2$ randomly, for $i = 1, 2, \dots, N$. The errors of interpolation are reported in Figure 7 and Figure 8 for u_1 and u_2 , respectively. In these figures, $N = 441$ HP (left) and UGP (right) are considered for interpolation. From these figures, the accuracy of the polynomial basis functions $p_{i,2}$ and $q_{i,2}$ are almost independent of the distribution of center points, while common polynomial basis functions are very sensitive to it. On the other hand, from the condition number of the coefficient matrix Φ , plotted in Figure 9, it is clear that the new proposed polynomial basis functions are more stable than conventional ones, specially for UGP center points.

From Figures 7 and 8 one can see, that the accuracy of the proposed polynomial basis functions is more than the common ones. It is notable that, from these figures, the proposed polynomials are more accurate than GA RBFs in approximating u_1 for each value of ε , while they are less accurate than the RBFs for interpolating u_2 when $\varepsilon = 1.5$. This is valid because u_1 is smoother than u_2 and polynomials can

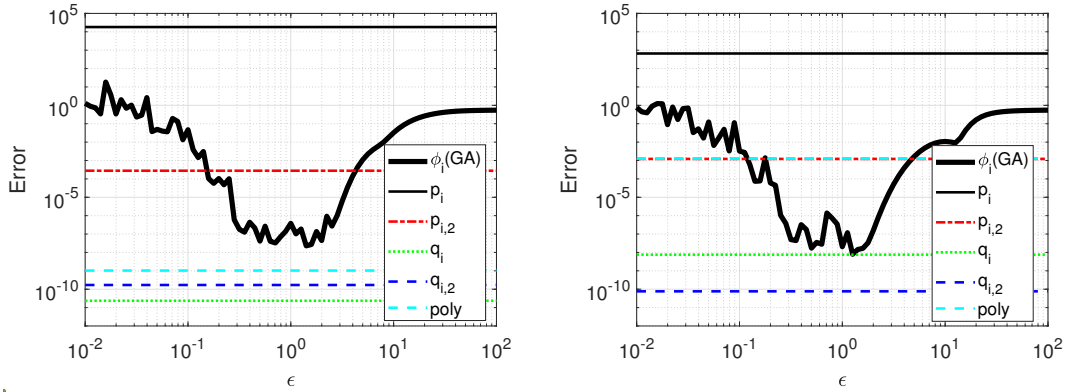


Figure 7: The RMSE for interpolating u_1 by polynomial basis functions $p_i, p_{i,2}, q_i, q_{i,2}$, common polynomials (poly) and GA RBF ($\phi_i(GA)$) versus shape parameter ϵ . The interpolation points are considered HP and UGP for the left and right pictures, respectively. Also, the number of interpolation points is $N = 441$.

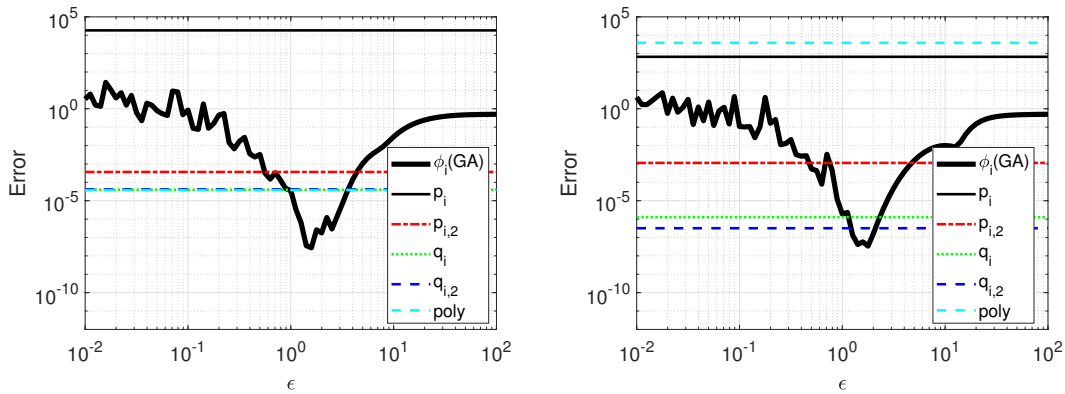


Figure 8: The RMSE for interpolating u_2 by polynomial basis functions $p_i, p_{i,2}, q_i, q_{i,2}$, common polynomials (poly) and GA RBF ($\phi_i(GA)$) versus shape parameter ϵ . The interpolation points are HP and UGP for the left and right pictures, respectively. Also, the number of points is $N = 441$.

approximate it more accurately. Figures 7 and 8 verify this claim, as the error of polynomial interpolation reported in these figures is less than 10^{-10} and 10^{-5} for u_1 and u_2 , respectively. These figures show polynomial basis functions $q_{i,2}$ are appropriate alternatives for the RBFs to approximate scattered data when the unknown function is smooth. The same investigation is done for the irregular domain (star-shaped domain) illustrated in Figure 10.

Functions u_1 and u_2 again are interpolated by the polynomials and GA RBF, that are introduced previously, at $N = 121$ scattered points, and RMSE (21) is calculated for them. The errors of u_1 and u_2 are reported in Figure 11 left and right, respectively. This figure reveals that the accuracy of regularized polynomial basis functions q_i and $q_{i,2}$ is significantly higher than the GA RBF.

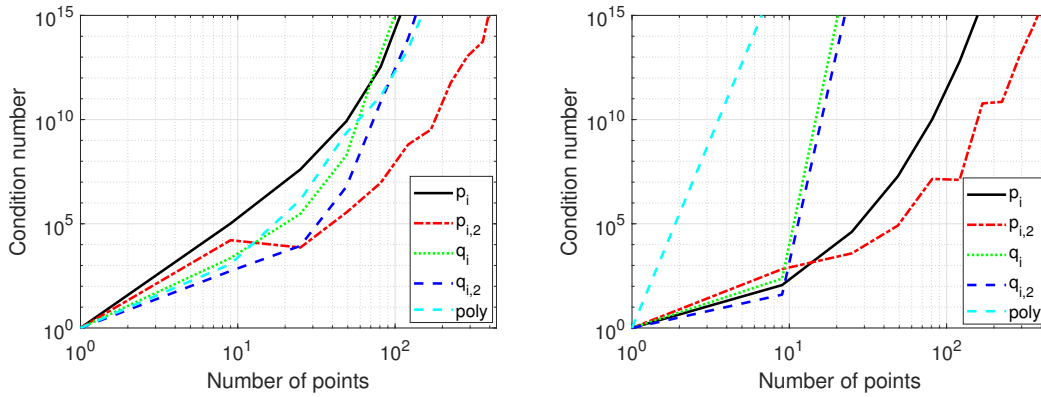


Figure 9: The condition number of the coefficient matrices, that are made by p_i , $p_{i,2}$, q_i , $q_{i,2}$, and common polynomials (poly) versus the number of center points. The left and right figures concerning HP and UGP center points.

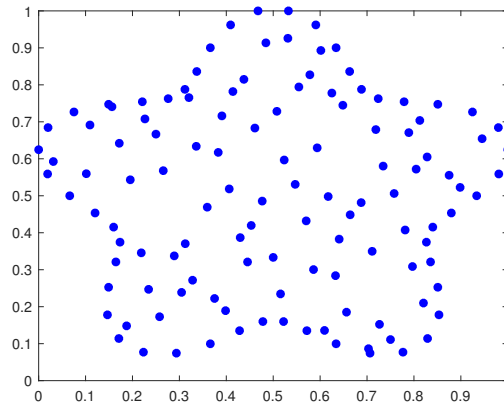


Figure 10: HP considered on the irregular domain.

5.2.2 3D domain

The polynomial basis functions also are applied to interpolate three-dimensional data points demonstrated in Figure 12 (left).

In this case study, $N = 1331$ HP are selected in $[-1, 1]^3$ as interpolation points, and the error of interpolation is calculated by RMSE formulation (21) when the exact solution is

$$u(x, y, z) = \sin(x + y + z).$$

The error is shown in Figure 12 (right) and it reveals that regularized basis functions q_i and $q_{i,2}$ are significantly more accurate than that of the other polynomial and GA RBF.

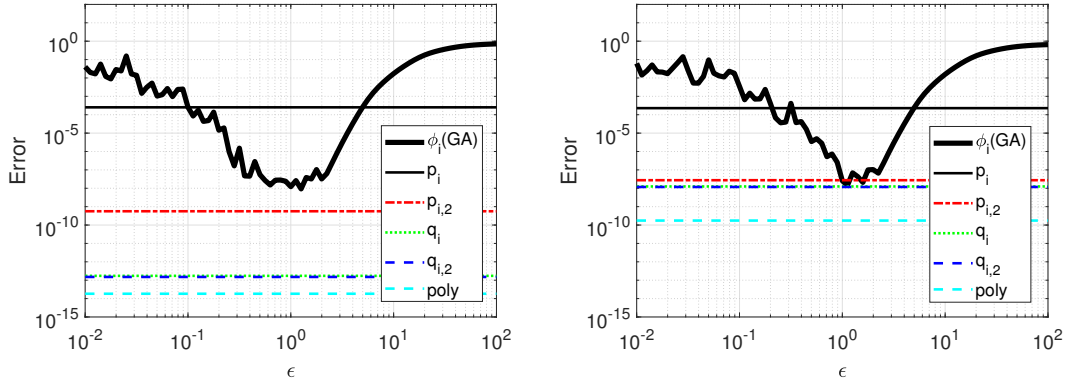


Figure 11: The RMSE for interpolating u_1 (left) and u_2 (right) by polynomial basis functions p_i , $p_{i,2}$, q_i , $q_{i,2}$, common polynomials (poly) and GA RBF ($\phi_i(GA)$) versus shape parameter ε for the stare shape. The number of points is $N = 121$.

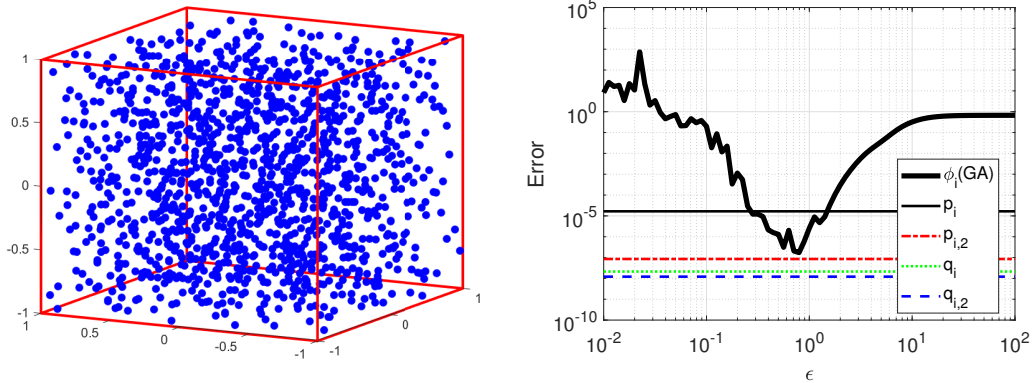


Figure 12: The interpolation points for the cube domain (left) and the RMSE of the interpolation (right) for the polynomial and radial basis functions versus shape parameter ε .

6 Conclusion and final remarks

Motivated by Taylor’s expansion of infinitely smooth RBFs, a new linear space of shifted radial polynomials of degree $2n$, denoted by \mathcal{H}_n , was proposed. For analysis, a set of basis functions was obtained for \mathcal{H}_n and its dimension was specified. Then, some important relations between \mathcal{H}_n and the linear space of polynomials of degree $2n$, \mathcal{P}_{2n} were found. It was shown that the distance between RBFs to both \mathcal{H}_n and \mathcal{P}_{2n} are numerically equal. Therefore, since for $d \geq 2$, \mathcal{H}_n is considerably smaller than \mathcal{P}_{2n} , it can be used for efficiently approximating RBFs. Two more appropriate basis functions were proposed for \mathcal{H}_n to enhance its numerical efficiency. The fast convergence of the proposed polynomial space to RBFs suggests it is an alternative to smooth RBFs for scattered data interpolation. In future works, the authors suggest finding new orthogonal or compact support polynomial basis functions for \mathcal{H}_n . Also, the properties of the proposed polynomial space can be used to find an optimal value for shape parameters in smooth RBFs.

Acknowledgements

The authors are thankful to the reviewers for their valuable feedback, which greatly enhanced the quality of the paper. Also, they appreciate Professor Ahmad Shirzadi and Elisabeth Larsson for their advice to increase the quality of this work.

References

- [1] D. Chen, *Research on traffic flow prediction in the big data environment based on the improved RBF neural network*, IEEE Trans. Ind. Inform. **13** (2017) 2000–2008.
- [2] T.A. Driscoll, B. Fornberg, *Interpolation in the limit of increasingly flat radial basis functions*, Comput. Math. Appl. **43** (2002) 413–422.
- [3] G.E. Fasshauer, *Meshfree Approximation Methods with MATLAB*, World Scientific, 2007.
- [4] B. Fornberg, N. Flyer, *A Primer on Radial basis Functions with Applications to the Geosciences*, SIAM, 2015.
- [5] B. Fornberg, E. Larsson, N. Flyer, *Stable computations with Gaussian radial basis functions*, SIAM J. Sci. Comput. **33** (2011) 869–892.
- [6] B. Fornberg, E. Lehto, C. Powell, *Stable calculation of Gaussian-based RBF-FD stencils*, Comput. Math. Appl. **65** (2013) 627–637.
- [7] B. Fornberg, C. Piret, *A stable algorithm for flat radial basis functions on a sphere*, SIAM J. Sci. Comput. **30** (2007) 60–80.
- [8] B. Fornberg, G. Wright, *Stable computation of multiquadric interpolants for all values of the shape parameter*, Comput. Math. Appl. **48** (2004) 853–867.
- [9] B. Fornberg, G. Wright, E. Larsson, *Some observations regarding interpolants in the limit of flat radial basis functions*, Comput. Math. Appl. **47** (2004) 37–55.
- [10] B. Fornberg, J. Zuev, *The Runge phenomenon and spatially variable shape parameters in RBF interpolation*, Comput. Math. Appl. **54** (2007) 379–398.
- [11] P. Gonzalez-Rodriguez, M. Moscoso, M. Kindelan, *Laurent expansion of the inverse of perturbed, singular matrices*, J. Comput. Phys. **299** (2015) 307–319.
- [12] R. L. Hardy, *Multiquadric equations of topography and other irregular surfaces*, Journal of geophysical research, **76** (1971) 1905–1915.
- [13] M.K. Esfahani, A. Neisy, S. De Marchi, *An RBF approach for oil futures pricing under the jump-diffusion model*, J. Math. Model. **9** (2021) 81–92.
- [14] E. Larsson, B. Fornberg, *Theoretical and computational aspects of multivariate interpolation with increasingly flat radial basis functions*, Comput. Math. Appl. **49** (2005) 103–130.

- [15] W.R. Madych, *Miscellaneous error bounds for multiquadric and related interpolators*, Comput. Math. Appl. **24** (1992) 121–138.
- [16] M. Mongillo, *Choosing basis functions and shape parameters for radial basis function methods*, SIAM undergraduate research online, **4** (2011) 190–209.
- [17] R. Schaback, *Error estimates and condition numbers for radial basis function interpolation*, Adv. Comput. Math. **3** (1995) 251–264.
- [18] R. Schaback, *Multivariate interpolation by polynomials and radial basis functions*, Constr. Approx. **21** (2005) 293–317.
- [19] F. Soleymani, Sh. Zhu, *Error and stability estimates of a time-fractional option pricing model under fully spatial-temporal graded meshes*, J. Comput. Appl. Math. **425** (2023) 115075.
- [20] H. Wendland, *Scattered Data Approximation*, Cambridge University Press, 2004.
- [21] G. B. Wright, B. Fornberg, *Stable computations with flat radial basis functions using vector-valued rational approximations*, J. Comput. Phys. **331** (2017) 137–156.
- [22] Y. Wu, X. Sun, *Optimization and simulation of enterprise management resource scheduling based on the radial basis function (RBF) neural network*, Comput. Intell. Neurosci. **2021** (2021) 6025492